Efficient Organic Electroluminescent Devices Using Single-Layer Doped Polymer Thin Films with Bipolar Carrier Transport Abilities

Chung-Chih Wu, James C. Sturm, Richard A. Register, Jing Tian, Elena P. Dana, and Mark E. Thompson

Abstract—Detailed studies of electroluminescent devices made from single-layer doped polymer blend thin films having bipolar carrier transport abilities are presented. The active organic layer consists of the hole-transport polymer poly(N-vinylcarbazole) (PVK) containing dispersed electron-transport molecules, as well as different fluorescent small molecules or polymers as emitting centers to vary the emission color. Both the photoluminescence and electroluminescence (EL) properties are extensively studied. In photoluminescence, very efficient transfer of energy can occur from the host to very dilute ($\sim$1 wt.%) amounts of emitting materials. When covered with a metal layer, the intensity of photoluminescence from blend thin films was found to be dependent on the type of metal coverage. The optical and electrical properties of materials and devices were systematically studied to understand the operating mechanisms and to optimize the devices. In EL, excitons appear to be formed at doped emitting centers, rather than in the host. We show that in an optimized device, a relatively high external quantum efficiency ($>$1%, backside emission only) and a low operating voltage ($<$10 V for over 100 cd/m^2) can be easily achieved by this class of devices. It was also found air-stable Ag is as good as reactive Mg : Ag alloy for the cathode contact in devices using PVK containing dispersed electron-transport oxadiazole molecules.

I. Introduction

IN RECENT years, there has been a high level of interest in polymer-based organic light-emitting devices (OLED's). The ability to form thin films of polymers from solutions by convenient wet coating techniques allow them to be deposited on many kinds of substrates, providing opportunities for many novel applications [1]–[6]. The ease of fabrication in comparison with inorganic devices is an attractive advantage of organic devices. The inherent thin-film structures and reasonable performance of devices make them particularly attractive for flat panel display applications, either as backlighting sources or directly as emitters in emissive displays [7]–[9].
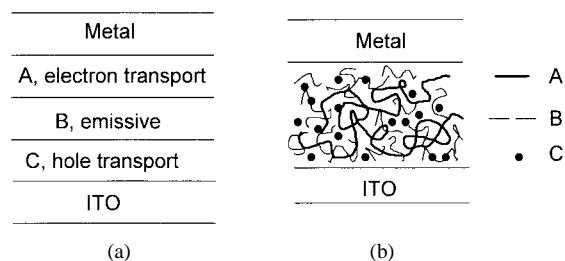
Fig. 1. Comparison of (a) an organic EL device with the layered structure, and (b) an organic EL device with a single-layer polymer blend thin film.

However, many electroluminescent polymers have only unipolar injection/transport ability. A luminescent polymer rarely has both good hole and electron transport or injection abilities with available anodes and cathodes. Therefore, it is often desired to have a hole injection/transport layer adjacent to the anode and/or an electron injection/transport layer adjacent to the cathode, with the emitting layer in the middle of the sandwich as shown in Fig. 1(a), to improve device performance [10]–[12]. With polymers, however, the formation of such multilayer structures is in general difficult. Extreme care has to be taken with respect to the solvents carrying different layers of materials, so that the solvent carrying a following layer will not dissolve the layers already deposited [11], [13].

Since the polymer thin films are typically coated from solutions, instead of forming multilayers, an alternative method to incorporate the functions of different materials into a thin film is to mix all electron-transport, hole-transport, and emissive materials together in a single solvent and then spin-coat the mixture in a single step, greatly simplifying the fabrication. Such a structure is known as a blend and is illustrated in Fig. 1(b). This is a peculiar advantage of polymers, resulting from their solution processability, and there is no analog of a blend structure for conventional inorganic semiconductors. In a blend, one hopefully preserves the hole transport, electron transport, and emissive properties of different materials, despite the fact that they are no longer layered but intimately mixed throughout the film. All these components need not be polymers, but at least one must be a polymer to bind all of the materials together. In our work, up to two molecular materials were used along with polymers. By changing the emitting materials, one should be able to tune the emission color. Several researchers have demonstrated devices
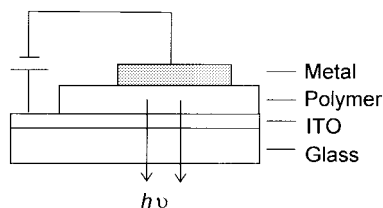
Fig. 2. Device configuration of a polymer EL device. A positive voltage is applied to ITO relative to the top metal contact under forward bias.

Fig. 3. Chemical structures of the materials used in this work.

made by this method [11], [14]–[18]. Due to its excellent film-forming property, the hole-transport polymer PVK has often been used as the matrix polymer, into which electron transport molecules and emitting dyes or polymers were dispersed. However, in most of these devices, the operating voltage is high, up to 30 V for light output to be visible [11], [14]–[16]. Also, for most of them, electroluminescence (EL) quantum efficiencies are modest, usually on the order of 0.1% (photon/electron). Furthermore, detailed characterization of this class of devices have not been performed. In this paper, we present the information relating to the optimization of this class of devices by systematically studying the relation between the device performance and the ratios of components in the blend. In contrast to most of the previous work, we found that devices can be made from these blend materials with a turn-on voltage of only 2–3 V and an operating voltage lower than 10 V at practical brightnesses. The external EL efficiency can exceed 1% (photon/electron), even with an air-stable metal cathode. By correlating device characteristics and material properties, we also seek to understand the behaviors of carriers inside these devices.

II. EXPERIMENTAL DETAILS

The device configuration employed is shown in Fig. 2, in which a thin film of the hole-transport matrix polymer PVK containing dispersed electron-transport molecules and luminescent materials is the only active organic layer. Fig. 3 lists the chemical structures of the organic materials used in the devices. The hole-transport polymer PVK, having a high weight-average molecular weight M_w of 1 100 000 g/mole reported by the supplier, was purchased from Aldrich Chemical Inc. and used as received. Electron-transport molecules, 2-(4-biphenyl)-5-(4-tert-butylphenyl)-1,3,4-oxadiazole (PBD), 2,5-bis(4-naphthyl)-1,3,4- oxadiazole (BND) and tris(8-hydroxyquinoline)aluminum (Alq) were purchased from Aldrich Chemical Inc., Lancaster Synthesis Inc., and TCI America, respectively. Several luminescent materials were used, including a conjugated polymer poly(3-n-butyl-p-pyridyl vinylene) (Bu–PPyV) and organic dyes: coumarin 6 (C6), coumarin 47 (C47), and nile red. Bu–PPyV was synthesized by cross-coupling the corresponding 2,5-dibromopyridine and E-1,2-bistributylstannylethylene in the presence of a palladium catalyst. The details of synthesis and its photophysical properties were reported elsewhere [19]–[22]. M_w was determined to be 5000–7000 g/mole by gel permeation chromatography ($M_w/M_n = 1.9$). Green dye C6 and the blue dye C47 were purchased from Lambda
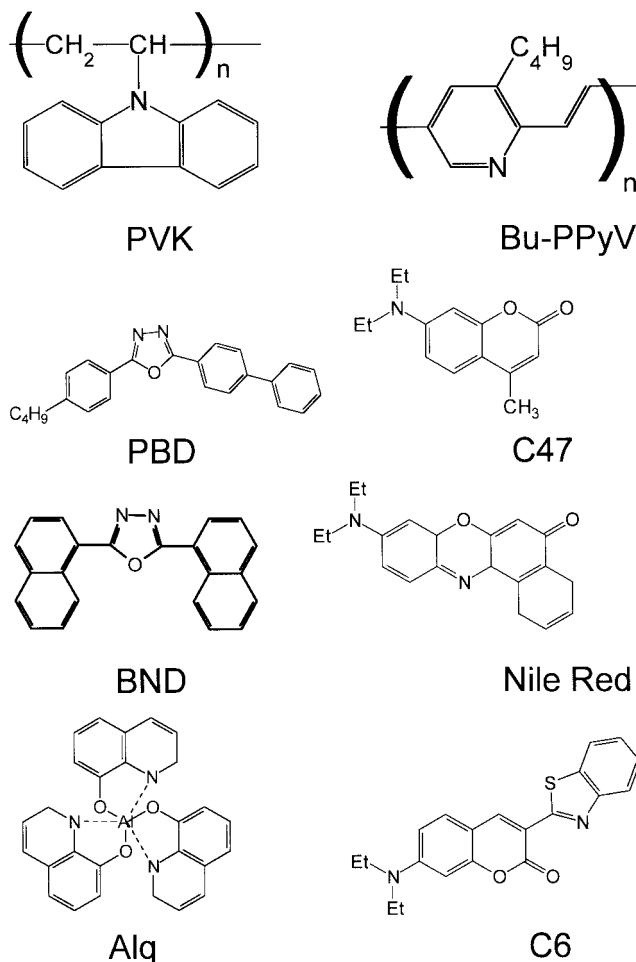
Physik Inc. Nile red was purchased from Aldrich. Chloroform solutions containing different amounts of PVK, electron-transport molecules and luminescent materials were prepared by stirring and were passed through 0.45-μm filters. Thin films of blends were spin-coated onto quartz slides for optical measurements and onto indium-tin-oxide (ITO)-coated glass substrates (1400 Å ITO, 11 $\Omega/\square$, purchased from Applied Films Corporation, Boulder, CO) for device fabrication. The ITO-coated glass substrates were carefully cleaned and pretreated with oxygen plasma before the coating of blend thin films [23]. Film thicknesses were controlled by the solution concentration and the spin rate, and were calibrated by an ellipsometer on reflective Si substrates. Typical spin rates used were 3000–5000 r/min. Uniform, dense, and pinhole-free films of 800–2000 Å were routinely achieved with a repeatability of $\pm$25 Å.

After spin-coating, samples were loaded into a vacuum chamber with a base pressure of $<10^{-6}$ torr for the metallization step of device fabrication. Typically, at least $\sim$90 min were allowed between the loading of samples and metal evaporation, and no further heating of samples was done. Top metal contacts were deposited through a shadow mask to form an array of 2 mm $\times$ 2 mm devices. Metal alloys, such as Mg : Ag (10 : 1) were deposited by coevaporation from two separate sources, followed by the deposition of

Ag the protection layer. All spin-coating, device processing, including direct loading into the evaporator for metallization, and device characterization were carried out under dry nitrogen atmosphere in a glove box.

Absorption and photoluminescence (PL) spectra of thin films were measured on an AVIV 14DS spectrophotometer and a Perkin–Elmer LS50 luminescence spectrometer, respectively. The EL spectra were recorded by an EG&G monochromator connected to an Electrim CCD camera. The light–current–voltage characteristics of the devices were measured using a Hewlett-Packard 4145B analyzer and a Si photodetector. The external EL quantum efficiency of devices was measured using a large-area (1 cm diameter) silicon photodetector, placed close to the bottom of the glass substrate. The measured photocurrent was corrected only for detector efficiency. No further corrections were made for absorption, waveguiding in the glass substrate or other effects that act to decrease the light emitted out of the backside of the glass substrate. Thus, all the quantum efficiencies reported here represent the lower limits on the true external quantum efficiency. The luminance (cd/m^2) of OLED's was converted from the radiant power by assuming an angular distribution of Lambertian emission [24].

The reduction and oxidation potentials of materials were determined by electrochemical measurements on a PAR Potentiostat/Galvanostat Model 283. Pt wire was used as the working electrode and the counter electrode. Ag/AgCl served as a reference electrode. Polymers Bu–PPyV and PVK were coated from their solutions in tetrahydrofuran and dichloromethane, respectively, onto the Pt working electrode, and electrochemical measurements were performed with the films immersed into the supporting electrolyte solutions (0.05 M tetrabutylammonium hexafluorophosphate (TBAHFP) in DMSO for Bu–PPyV and 0.2 M LiClO$_4$ in acetonitrile for PVK). Other compounds were used as molecular solutions in DMSO containing 0.05 M tetramethylammonium tetrafluoroborate (TMA TFB) or acetonitrile containing 0.2 M LiClO$_4$. Oxygen was removed from the working solutions by bubbling with argon gas of highest purity. The measured redox potentials versus Ag/AgCl were later converted to potentials versus ferrocene–ferrocenium (FOC) redox couple by including the potential difference between FOC and Ag/AgCl in the same solutions.

III. CHARACTERISTICS OF THE PVK : Bu–PPyV AND PVK : PBD : Bu–PPyV BLENDS

A. Optical Properties of Blend Thin Films

In this paper, we will use the PVK : Bu–PPyV and PVK : PBD : Bu–PPyV blends as model systems for detailed discussions. The conclusions drawn from this model system can be generalized to other material systems in this paper when appropriate. Fig. 4 shows the absorption spectra of thin films of PVK, PBD, Bu–PPyV, and their mixtures. Clearly, both PVK and PBD have shorter absorption onset wavelengths than Bu–PPyV and therefore higher optical energy gaps. The absorption spectra of their mixtures can be fitted by weighted

superpositions of the spectra of the individual components, indicating no ground state interaction between materials. Since Bu–PPyV was added into the PVK or PVK : PBD host to act as the emitting centers, we were then interested in its emission behavior in the host. In exciting the thin films, two excitation wavelengths, 340 and 420 nm, were used to extract different information about the optical properties of the blend thin films. The 420-nm wavelength is used because it is close to the absorption peak of Bu–PPyV and is below the absorption onset energy of PVK and PBD. By exciting the thin films at 420 nm, only Bu–PPyV chromophores are excited. The 340-nm wavelength is used because its photon energy is beyond the PVK and PBD absorption onset energies and there is minimal absorption from Bu–PPyV. The PL spectra of PVK : Bu–PPyV thin films with different Bu–PPyV contents using an excitation wavelength of 420 nm are shown in Fig. 5(a). In blends with low Bu–PPyV contents, a strong green emission is observed. When the Bu–PPyV content increases above several percent, the PL spectra gradually become broadened and shift to the red. The same evolution of PL was observed for the PVK : PBD : Bu–PPyV three-component system. By normalizing the integrated PL intensity by the absorption of the same blend film at 420 nm, the relative PL efficiencies of Bu–PPyV chromophores diluted in PVK or PVK : PBD are obtained and displayed in Fig. 5(b). The efficient green PL in blends with low Bu–PPyV contents arises in the emission of isolated Bu–PPyV chromophores, while the weak red PL in blends with high Bu–PPyV contents and pure Bu–PPyV thin films is from Bu–PPyV excimer emission. Excimers form due to the strong interaction between Bu–PPyV chromophores. The PL efficiency starts dropping rapidly around 2 wt.% Bu–PPyV. It is clear that diluting Bu–PPyV with the high energy gap PVK eliminates the interaction between Bu–PPyV chromophores and maintains the high PL efficiency of isolated Bu–PPyV chromophores, indicating that the Bu–PPyV and PVK chains are molecularly mixed. Similar emission spectra and behaviors were also observed in the tetrahydrafuron (THF) solutions of Bu–PPyV at various concentrations [22], precluding the possibility that the emission is from a complex between Bu–PPyV and PVK or PBD in the excited state, such as a charge-transfer complex exciplex, which also usually leads to a shift of emission toward lower energies as well as a decrease in luminescence efficiency. The exciplexes are analogous to the spatially indirect excitons formed at the interface of two inorganic semiconductor layers with Type II band alignment. The exciplexes between Bu–PPyV and PVK or PBD are not expected on the basis of their redox properties, which are listed in Table I and will be discussed below.

With 420-nm excitation wavelength, excitons are formed only on Bu–PPyV chromophores, so the emission behavior of the Bu–PPyV chromophore itself in PVK or PVK : PBD matrix is investigated. On the other hand, by exciting into the absorption range of higher energy gap PVK and PBD using 340-nm excitation, the energy transfer between materials is probed. Fig. 6(a) plots the PL spectra of various PVK : Bu–PPyV blends using 340-nm excitation. With the Bu–PPyV content as low as 1 wt.%, almost all emission is from Bu–PPyV even though almost all excitation energy

TABLE I

ELECTROCHEMICAL POTENTIALS AND ENERGY LEVELS OF MATERIALS. ELECTROCHEMICAL POTENTIALS WERE MEASURED BY CYCLIC VOLTAMMETRY.
HOMO AND LUMO LEVELS WERE CONVERTED FROM MEASURED ELECTROCHEMICAL POTENTIALS ASSUMING THE ABSOLUTE ENERGY LEVEL OF
FOC TO BE −4.8 EV. VALUES MARKED BY * WERE ESTIMATED FROM MEASURED HOMO OR LUMO LEVELS AND OPTICAL ENERGY GAPS

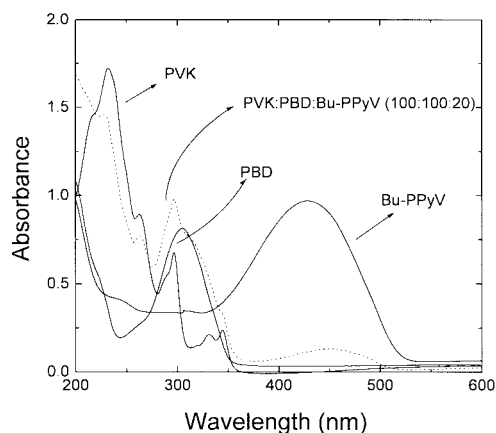| Materials	Oxidation Potential (V vs. FOC)	Reduction Potential (V vs. FOC)	Optical Energy Gap (eV)	HOMO (eV vs. vacuum)	LUMO (eV vs. vacuum)
PVK	0.74		3.5	-5.54	-2.04*
Bu–PPyV		-1.87	2.45	-5.38*	-2.93
C6	0.59		2.46	-5.39	-2.93*
C47	0.57		2.88	-5.37	-2.49*
Nile Red	0.5	-1.31		-5.3	-3.49
PBD		-2.34	3.6	-6.06*	-2.46
BND		-2.16	3.3	-5.94*	-2.64
Alq	0.89		2.7	-5.69	-2.99*

Fig. 4. Absorption spectra of PVK, PBD, Bu–PPyV, and PVK : PBD : Bu–PPyV (100 : 100 : 20 by wt.)

is absorbed by PVK. A similar transition in emission was also observed between PVK : PBD and Bu–PPyV in the PVK : PBD : Bu–PPyV blends. Therefore, we can conclude that excitons formed in PVK or PVK : PBD of the blends efficiently transfer to Bu–PPyV chromophores. Such a transfer is presumably due to the lower energy gap of the Bu–PPyV. The emission from other components can only coexist with Bu–PPyV emission at extremely low Bu–PPyV content. The relative PL efficiency as a function of Bu–PPyV concentration is displayed in Fig. 6(b). For both PVK : Bu–PPyV and PVK : PBD : Bu–PPyV systems, there is modest enhancement of PL using 340-nm excitation in comparison with the PVK or PVK : PBD host without Bu–PPyV, by a factor of roughly 2 around 1–2 wt.% Bu–PPyV, indicating the small amount of Bu–PPyV doped into the PVK or PVK : PBD provides a more efficient radiative recombination channel for excitons.

B. Effects of Metal Coverage on PL of Blend Thin Films

There are always concerns regarding the effects of dielectric or metal coatings on the luminescence of organic thin films. Here we report the luminescence of organic blend thin films covered by different metals. The setup for the PL measurement is shown in Fig. 7. Films were coated on quartz or ITO/glass, with different metals deposited on top of the organic films. For each setup, there was one control sample without metal deposition. To assure that the films are in the same optical
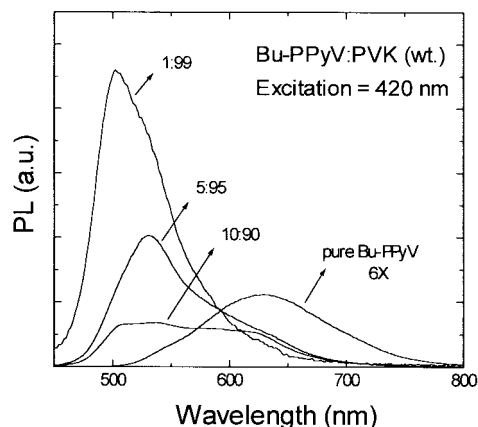
(a)
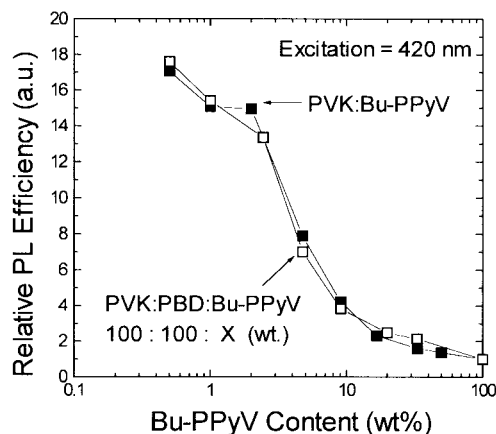
(b)

Fig. 5. (a) Photoluminescence spectra of Bu–PPyV : PVK blend thin films with different Bu–PPyV content. The excitation wavelength was 420 nm, exciting only Bu–PPyV chromophores. (b) Relative integrated PL efficiency of Bu–PPyV chromophores versus Bu–PPyV content in the PVK : Bu–PPyV or PVK : PBD : Bu–PPyV blend thin films. The excitation wavelength was 420 nm. The strengths were normalized by the strength of the absorption at 420 nm in each film.

environment, for the control sample without metal coverage, a metal (Al) coated glass mirror was used in tight contact with the film. The PL spectra from films on quartz and on ITO/glass are displayed on Fig. 8(a) and (b). For both sets of samples, all the metal samples have lower PL efficiencies than the control samples, apparently indicating that the metal films
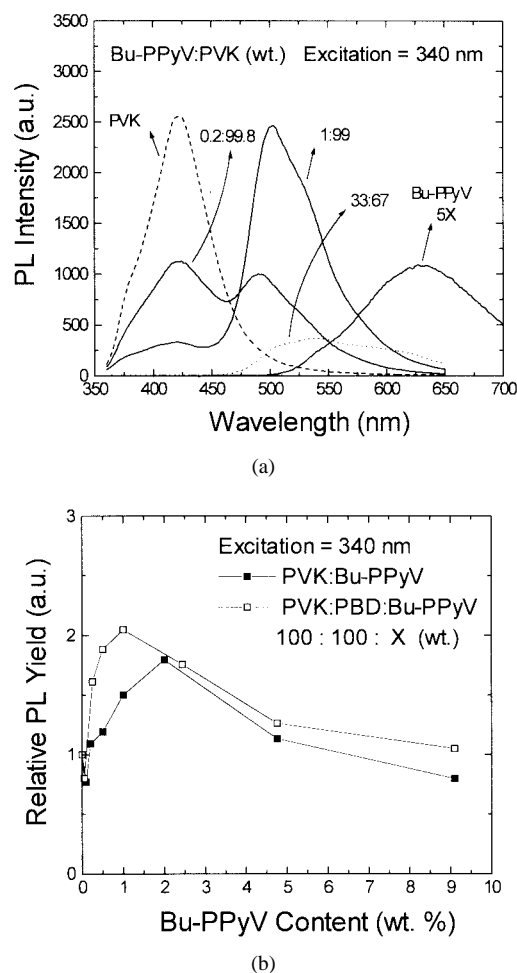
(a)

(b)

Fig. 6. (a) Photoluminescence spectra of Bu–PPyV : PVK blend thin films with different Bu–PPyV content. The excitation wavelength was 340 nm, with most absorption occuring in PVK as Bu–PPyV content is low. (b) Relative integrated photoluminescence efficiencies of PVK : Bu–PPyV and PVK : PBD : Bu–PPyV blend thin films versus Bu–PPyV content. The excitation wavelength was 340 nm. The strengths were normalized by the absorption at 340 nm in each film.

directly deposited onto the organic films do not just function as a mirror, like the metal mirror for the control sample. Furthermore, the luminescence intensity varies with the deposited metals. There are several reports and proposed explanations for the effects of metal coverages on the luminescence of organic thin films [25]–[28]. One is the optical interference theory [26], [28], in which the radiative lifetime (rate) of emitting species and the luminescence efficiency are dependent on the optical environment and the spacing between the emission zone and interfaces. Also, the metal overlayers on organic thin films could quench luminescence through several possible mechanisms [27], [29], [30]. First, energy level bending could cause field-induced luminescence quenching [29], [30]. Also, interaction between metals and organics could produce products or interface states which quench luminescence. Among the above, the contact quenching and energy level bending effects are particularly dependent on the metal deposited. From the device optimization point of view, a barrier/buffer layer with an appropriate carrier transport ability on top of the blend thin film may be required to prevent carriers from

recombination near the cathode metal contact or to control the spacing between the emission zone and the contact.

C. Electrochemical Properties of Materials Used in the Blends

In the organic guest-host system or doped carrier-transport polymers, we need to consider not only energy transfer, but also charge transfer or carrier trapping. These characteristics strongly depend on the electrochemical or redox properties of each individual component in the system. We therefore, measured the reduction and oxidation potentials of the materials used. The examples of typical cyclic voltammograms are shown in Fig. 9. The electrochemical potentials versus those of ferrocene/ferrocenium (FOC) redox couple measured in the same solution used for each material are listed in Table I. Assuming the energy level of FOC is 4.8 eV below the vacuum level, the absolute positions of the HOMO (highest occupied molecular orbital) and LUMO (lowest unoccupied molecular orbital) levels versus the vacuum level have been derived from these electrochemical levels [13], [31], and are also listed in Table I. For some materials, only reduction or oxidation potentials were successfully obtained, their HOMO or LUMO levels were estimated by subtracting the apparent optical energy gap (the absorption onset energy) from their LUMO levels or adding the apparent optical energy gap to their HOMO levels [13], [31]. HOMO levels or LUMO levels estimated this way were marked by an asterisk mark in Table I. We note that the oxidation potentials and the reduction potentials, of course, correspond to but do not necessarily exactly equal to the HOMO and LUMO levels [13], [31], [32], and the evaluation of HOMO and LUMO levels from the electrochemical data in combination with the optical energy gaps is still a matter of debate. However, one should still be able to extract the relative trend of the energy level alignment of HOMO's and LUMO's of different materials from these electrochemical potentials. According to the energy levels listed in Table I, the relative positions of energy levels of PVK, PBD, and Bu–PPyV are shown in Fig. 10. With such an energy level alignment, Bu–PPyV should be able to trap holes from hole-transport PVK or trap electrons from electron-transport PBD. Also, exciplexes between Bu–PPyV and PVK or PBD should not be expected as mentioned previously. Instead, energy transfer is allowed since the Bu–PPyV has a lower energy gap and its energy levels lie between those of PVK and PBD.

IV. OPTIMIZATION OF DEVICES USING BU–PPYV AS EMISSION CENTERS

A. PVK : Bu–PPyV Blends

In this section, we discuss the EL of three different structures: ITO/PVK : Bu–PPyV/Metal, ITO/PVK : PBD : Bu–PPyV/Metal and ITO/PVK : BND : Bu–PPyV/Metal. First, the PVK : Bu–PPyV system was studied. In general, in going from pure PVK to pure Bu–PPyV with the addition of Bu–PPyV, the EL of PVK : Bu–PPyV blends goes through the transition from deep blue PVK emission to green emission of isolated Bu–PPyV chromophores and then to
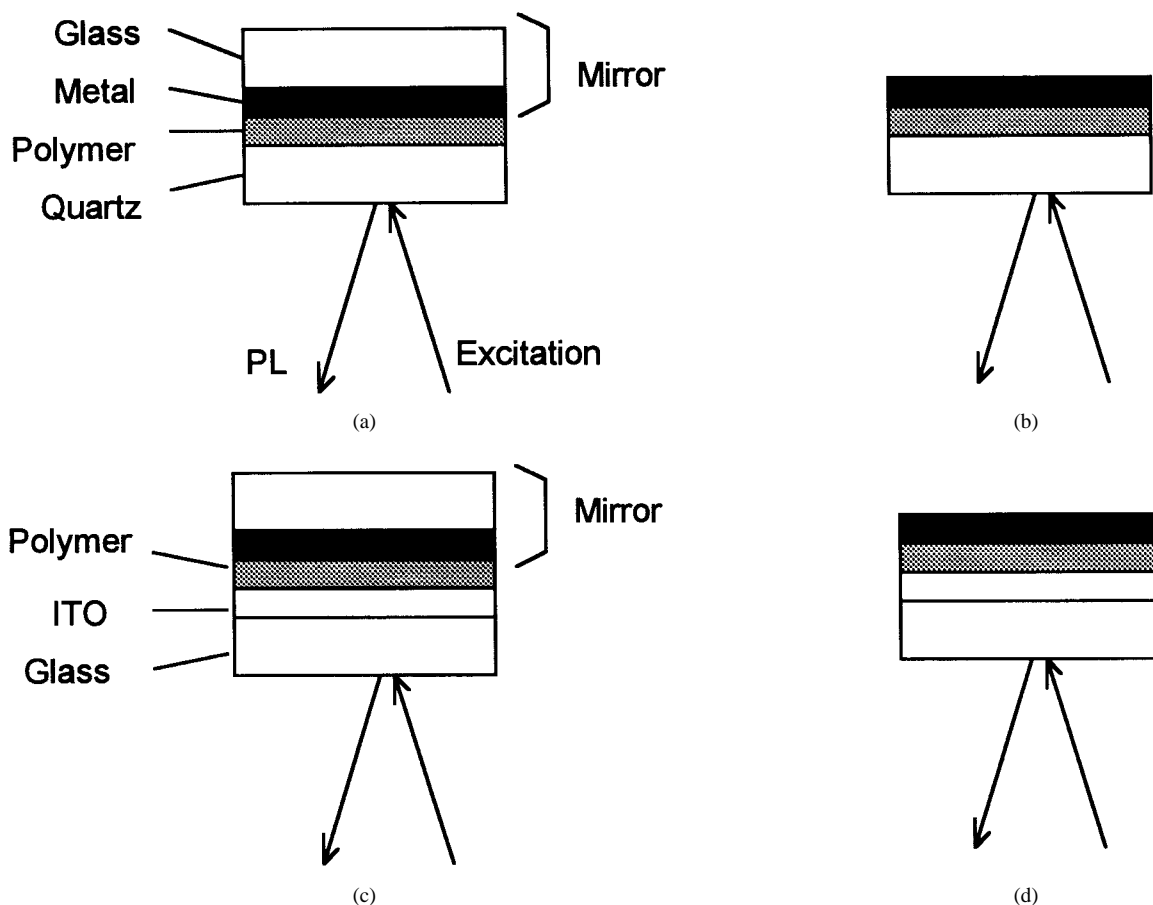
Fig. 7. PL measurement in various structures: (a) polymer thin film on quartz, in physical contact with an aluminum mirror, (b) polymer thin film on quartz, covered with a deposited metal layer, (c) polymer thin film on ITO, in physical contact with an aluminum mirror, and (d) polymer thin film on ITO, covered with a deposited metal layer. The polymer film is PVK : PBD : Bu–PPyV (100 : 100 : 2 by wt.) blend thin films of 110 nm. The excitation wavelength is 340 nm.

red emission of Bu–PPyV excimers, spanning the whole visible spectrum from this single series of blends as shown in the spectra of Fig. 11. Fig. 12 shows the color photographs of these devices. The dependence of external EL quantum efficiency on the content of Bu–PPyV in PVK : Bu–PPyV is shown in Fig. 13, along with the relative PL efficiency (340-nm excitation). The EL efficiency first increases rapidly with Bu–PPyV content from 0.03% (photon/electron) for pure PVK to 0.3% at 0.5 wt.% Bu–PPyV content. The following drop of EL efficiency with further addition of Bu–PPyV above 1 wt.% is due to the reduced PL efficiency for these emission centers as shown in Figs. 5(b) or 6(b). The large initial increase in EL efficiency (10 times), however, can not be accounted for simply by the modest increase in the PL efficiency of the host matrix PVK [~2 times in Fig. 6(b)] caused by doping with Bu–PPyV, in which we assume excitons are first formed on the host and then transferred to the more radiatively efficient Bu–PPyV centers. Instead, this indicates that the observed enhancement of EL efficiency is mostly due to a significant enhancement of carrier recombination on Bu–PPyV centers, suggesting the direct formation of excitons on Bu–PPyV centers by sequential trapping of oppositely charged carriers. The trapped or more localized electrons or holes on these centers can then more easily capture the opposite carriers and form charge-carrier pairs, followed by efficient radiative

recombination. This hypothesis is further supported by the difference between PL spectra [Fig. 6(a)] and EL spectra (Fig. 13) of PVK : Bu–PPyV blends at low Bu–PPyV content. For example, in PL using 340-nm excitation wavelength to create excitons in PVK, at 0.2 wt.% of Bu–PPyV most of luminescence is still from PVK, whereas in EL, at 0.1 wt.% of Bu–PPyV, Bu–PPyV luminescence already dominates since more efficient carrier recombination can take place directly on the Bu–PPyV centers in the case of EL.

B. PVK : PBD : Bu–PPyV and PVK : BND : Bu–PPyV Blends

The PVK is well known as a hole-transport polymer [33], with hole transport through the side-chain carbazole group and with only extremely limited electron-transport ability if any. Therefore, though there is a large enhancement of EL in PVK : Bu–PPyV compared with pure PVK, device performance is thought to still be limited by the electron injection/transport ability of PVK. First of all, the large unbalance between holes and electrons leads to inefficient utilization of carriers. Also, due to the unbalanced hole and electron transport properties in the single-layer PVK : Bu–PPyV devices, it is very possible that the recombination takes place very close to the organic/metal cathode interface, which itself could be a quenching site. To improve the electron injection/transport ability of the films, the electron-transport oxadiazole PBD was
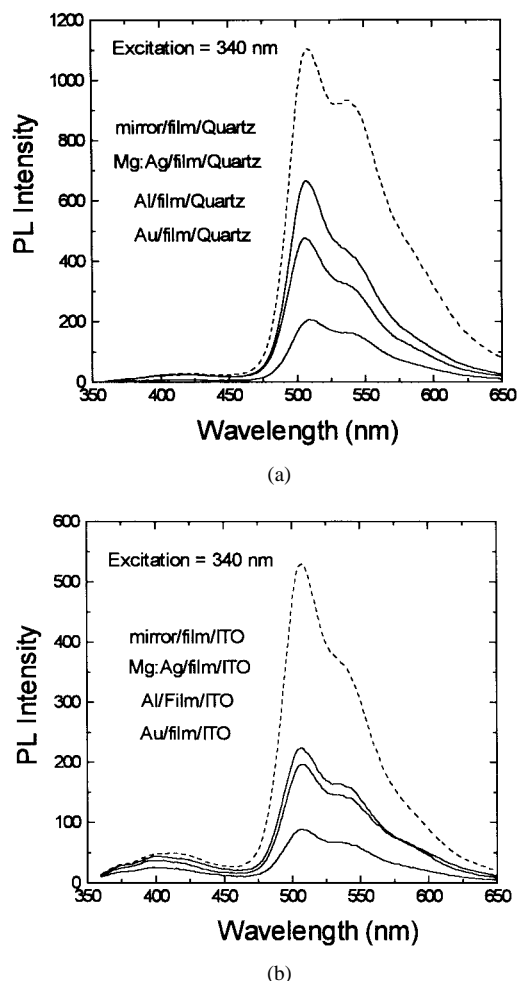
(a)

(b)

Fig. 8. (a) Measured PL intensity for structures (a) and (b) in Fig. 7 with various metal coverages. (b) Measured PL intensity for structures (c) and (d) in Fig. 7 with various metal coverages.
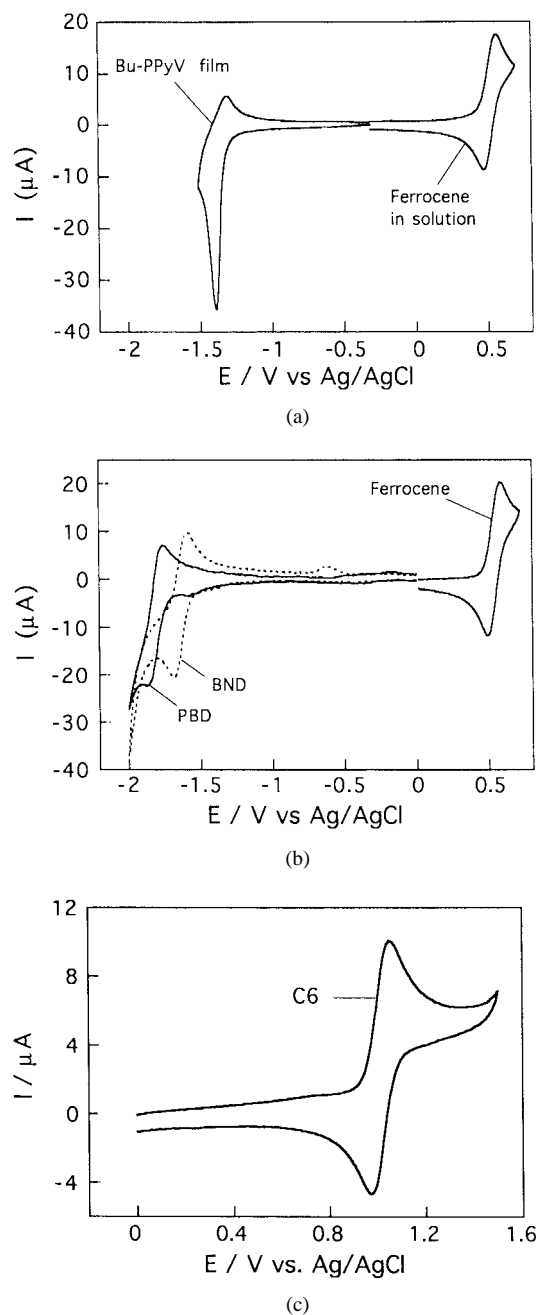

(a)

(b)

(c)

Fig. 9. Typical cyclic voltammograms from electrochemical spectroscopy. (a) Bu–PPyV as a film at the Pt working electrode, (b) PBD, BND, and (c) C6 as 5×10^{-4} M solutions. Supporting electrolytes: (a) 0.05 M tetrabutylammonium hexafluorophosphate (TBAHFP) in DMSO, (b) 0.05 M tetramethylammonium tetrafluoroborate (TMA TFB) in DMSO, and (c) 0.2 M LiClO$_4$ in acetonitrile. Potential scan rate was 0.1 V/s.

added. The external EL efficiency versus the Bu–PPyV content in PVK : PBD : Bu–PPyV system is shown in Fig. 14. The external EL efficiency versus the PBD content is shown in Fig. 15. As in the PVK : Bu–PPyV system shown in Fig. 13, the EL efficiency peaks for Bu–PPyV under 1 wt.%. The addition of PBD can further enhance the external EL efficiency severalfold compared to that without PBD, with the highest external EL efficiency of 0.8% achieved with a PVK to PBD ratio of about $100:40$–50 (by weight). Again, the large enhancement of EL with Bu–PPyV doping (~10 times) over PVK : PBD cannot be accounted for by the modest PL enhancement of the host, suggesting the same carrier trapping mechanism for EL enhancement as in the PVK : Bu–PPyV case. The difference between the EL and PL spectra again supports this hypothesis. In EL, no emission other than that of Bu–PPyV can be detected for Bu–PPyV contents as low as 0.05 wt.% in the PVK : PBD : Bu–PPyV blend thin film, while at that Bu–PPyV content, the emission from PVK : PBD dominates the PL. Therefore, in PVK : PBD : Bu–PPyV system, carrier trapping is an even more favored mechanism than the energy transfer.

The addition of PBD also has a tremendous effect on the forward $I–V$ characteristics of the devices, as shown in Fig. 16.

For all devices with identical thickness (1050 ± 25 Å), the rise of forward current with voltage first gets steeper with the PBD addition, leading to a reduction in the operating voltage of the devices. However, increasing the PVK : PBD weight ratio beyond $100 : 50$ does not further enhance the current. Instead, the $I–V$ curve is bent down again and the EL efficiency is reduced. Fig. 17 shows the effect of the addition of Bu–PPyV on the electrical characteristics of PVK : PBD : Bu–PPyV devices. With very low doping by Bu–PPyV (<1 wt.%), there is no significant change of the $I–V$ characteristics compared to
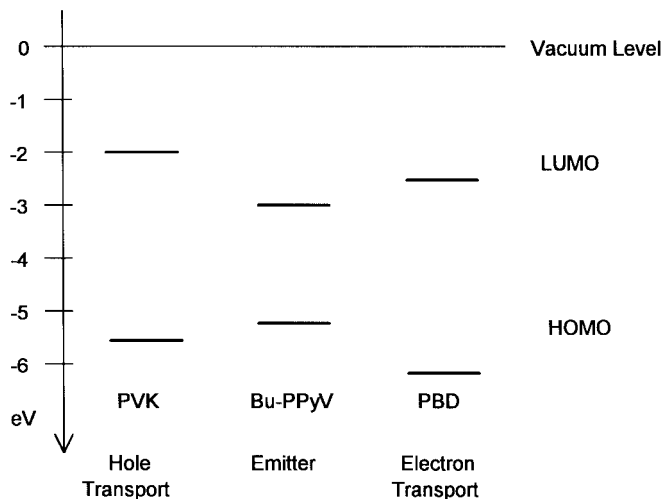
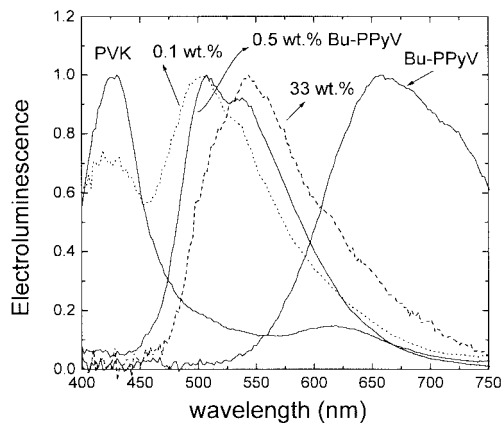Fig. 10. Relative energy level alignment for PVK, Bu–PPyV, and PBD according to the values listed in Table I.

Fig. 13. External EL efficiency of ITO/PVK : Bu–PPyV/Mg : Ag/Ag devices versus Bu–PPyV content. The relative PL efficiency (340 nm excitation) of PVK : Bu–PPyV blend thin films plotted in Fig. 6 is also shown for comparison.

Fig. 11. Normalized EL spectra of PVK : Bu–PPyV devices of different Bu–PPyV contents.

Fig. 14. External EL efficiency of ITO/PVK : PBD : Bu–PPyV/Mg : Ag/Ag devices versus Bu–PPyV content. PVK : PBD ratio is $100 : 50$ by wt. The relative PL efficeincy (340-nm excitation) of PVK : PBD : Bu–PPyV blend thin films plotted in Fig. 6 is also shown for comparison.
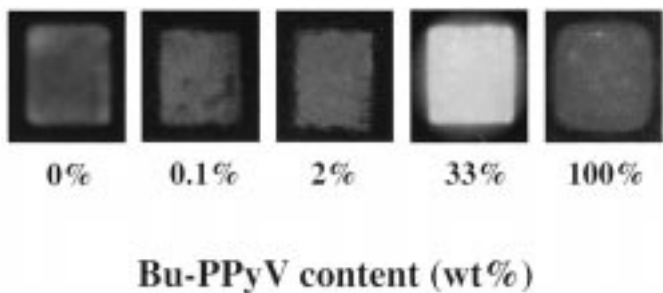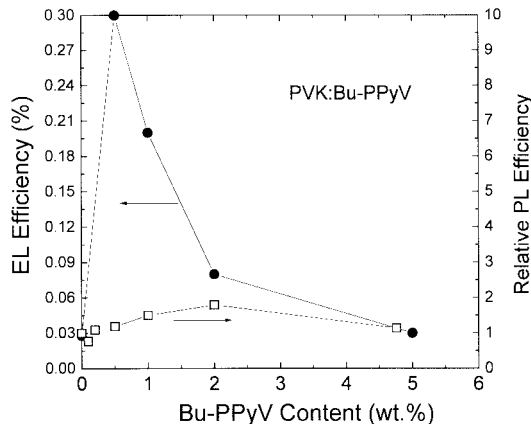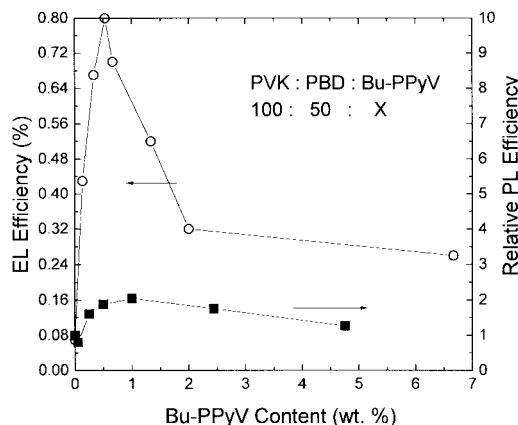

Fig. 12. The color photographs of working EL devices made from PVK : Bu–PPyV blend thin films of different ratios. Pure PVK devices emit purple-deep blue light. With extremely low Bu–PPyV content, the blend film emit blue-green light, a combination of PVK and isolated Bu–PPyV chromophore emissions. Green emission is from isolated Bu–PPyV chromophores. With higher Bu–PPyV content, the emission shifts to yellow and eventually to weak red emission of Bu–PPyV excimers.

Fig. 15. External EL efficiency of ITO/PVK : PBD : Bu–PPyV/Mg : Ag/Ag devices and ITO/PVK : BND : Bu–PPyV/Mg : Ag/Ag devices versus content of PBD or BND.

devices without Bu–PPyV doping. Therefore, there is no trade-off between the optimal doping for EL and keeping the operating voltage low. When the Bu–PPyV doping level is raised above 1 wt.%, the shift of I–V characteristics to higher voltages becomes significant, indicating that the carrier transport

properties of the host are perturbed by the doped Bu–PPyV. It is consistent with the lowering of carrier mobility in a carrier transport medium doped with carrier trapping centers.

Fig. 16. Forward *I–V* characteristics of ITO/PVK : PBD : Bu–PPyV/Mg : Ag/Ag devices of different PBD contents.
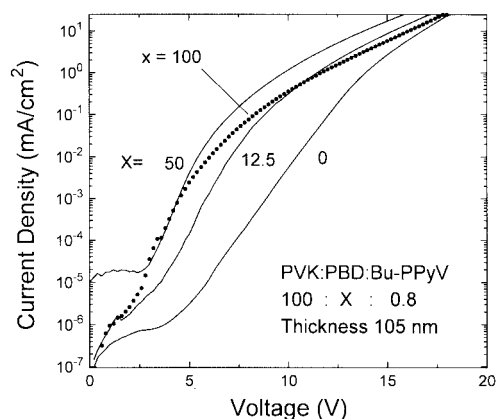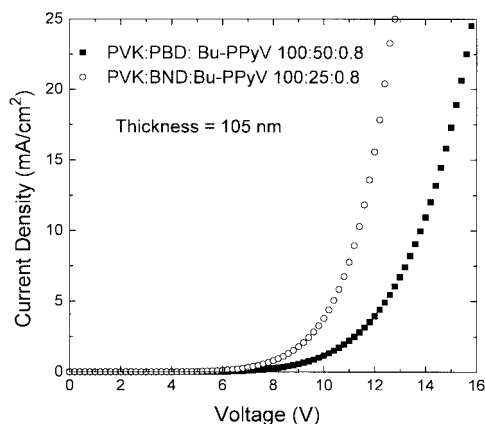

Fig. 18. Forward *I–V* characteristics of optimal ITO/PVK : PBD : Bu–PPyV/Mg : Ag/Ag and ITO/PVK : BND : Bu–PPyV/Mg : Ag/Ag devices.
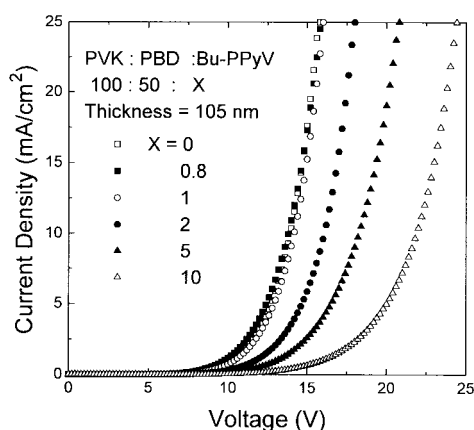

Fig. 17. Forward *I–V* characteristics of ITO/PVK : PBD : Bu–PPyV/Mg : Ag/Ag devices of different Bu–PPyV contents. PVK : PBD ratio is 100 : 50 by wt.

The dependence of EL on PBD content (Fig. 15) probably results from the combination of two effects: improved electron injection and improved electron transport as PBD is added. While improved electron injection improves the balance of carriers, the improved electron transport could move the major recombination zone away from the organic/cathode interface, reducing the metal contact quenching effect. We note that the electron mobility of PBD usually increases (rapidly) with its concentration in a polymer binder [34] while the hole mobility of PVK could be perturbed (i.e., reduced) by the additives [33], [35]. The optimal PVK : PBD ratio for EL could therefore be the tradeoff between hole injection/transport and electron injection/transport. That the lowest drive voltage occurs in the device with the highest quantum efficiency might be due to a larger carrier recombination current for better balanced carrier injection, although probably only a small portion of it contributes to EL, i.e., radiative recombination. When either hole or electron current is dominant, the balance of currents and therefore the carrier recombination is worse, leading to a higher voltage and lower EL efficiency. In addition, unbalanced carrier injection/transport could move the recombination zone closer to cathode or anode, resulting in luminescence quenching and lower EL efficiency.

These concepts were tested by replacing PBD with BND, another electron-transport oxadiazole molecule which has similar electrochemical properties to PBD but has a much higher electron mobility when dispersed in a polymer binder [34]. In this case, a stronger effect of electron transporter content on EL efficiency was observed. The comparison of the EL efficiencies of BND and PBD devices is made in Fig 15. Although it is plotted versus the weight ratios, molecular weights of BND and PBD are similar (322.37 versus 354.46). Though the optimal EL efficiency is about the same for both PBD and BND devices, the BND device is optimized at lower electron transporter content, with a steeper rise and falloff of the EL efficiency away from the optimum. Also, the optimal BND device requires a lower operating voltage than the optimal PBD devices, as shown in Fig. 18. We propose that the better electron injection/transport ability of BND leads to a balance of carrier injection/transport at lower content and steeper rise and falloff of EL efficiencies with BND content. Since less BND is required for optimization, the hole injection/transport of PVK is less perturbed, meaning that both better hole and electron injection/transport contribute to the lower operating voltage of the optimal BND device.

V. DEVICES USING ORGANIC DYES AS EMISSION CENTERS

A. Tuning of Colors

We have also explored the use of molecular dyes instead of Bu–PPyV as the emitting dopants. Since the emission from the blend is basically that of the emitting dopants, replacing Bu–PPyV with other centers which emit efficiently in different parts of the visible spectral range and have appropriate redox properties so that all materials have an energy level alignment similar to that in Fig. 8, would permit color tuning for EL devices. Since both PVK and oxadiazoles fluorescence at energies higher than blue light, color tuning up to blue light is possible. Fig. 19 shows the EL spectra of blue, green, and orange devices made from molecularly-doped PVK, with either PBD or Alq as electron-transport molecules. The emitting dopants used are commercial organic laser dyes or pigments, coumarin 47 (C47), coumarin 6 (C6)
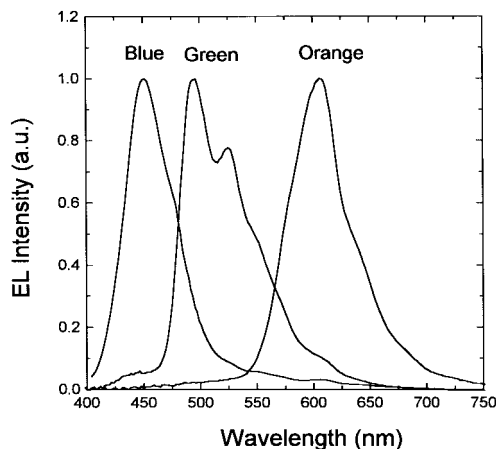
Fig. 19. EL spectra of blue, green, and orange devices, the compositions of which are ITO/PVK : PBD : C47(100 : 40 : 1 by wt.) /Mg : Ag/Ag, ITO/ PVK:PBD:C6 (100:40:0.3 by wt.)/Mg:Ag/Ag and ITO/PVK:Alq:nile red (100 : 40 : 0.2 by wt.)/Mg : Ag/Ag, respectively.

Fig. 20. Forward current–voltage–brightness characteristics of the blue ($\bigcirc$), green ($\blacksquare$), and orange ($\square$) devices in Fig. 19.

and nile red for blue, green and orange EL. The composition of each blend was optimized following the same strategy described in the previous section. The detailed compositions for the blue, green, and orange devices are PVK : PBD : C6 (100 : 40 : 1 by wt.), PVK : PBD : C6 (100 : 40 : 0.3 by wt.), and PVK : Alq : nile red (100 : 40 : 0.2 by wt.), respectively. Fig. 20 shows their corresponding I–V–L curves. All these devices have quite similar I–V characteristics. Currents start rising rapidly between 2 to 4 V, with light emission becoming detectable between 3 to 5 V, correspondingly. Other groups have reported similar PVK-based single-layer devices, but such low turn-on voltages have never been previously observed. With similar film thicknesses, the turn-on voltages of $\sim$3–5 V in our devices are much less than the turn-on voltages of $\sim$10–30 V in previous work [11], [14]–[16], [18]. The main obvious difference in our work is the improvement of the ITO anode contact to the blend OLED's via oxygen plasma treatment, which has been found to modify the surface composition and the surface work function [23]. The hole-injection efficiency and the performance of the single-layer doped polymer OLED's are thus substantially enhanced. In these devices, practical brightnesses of 10–100 cd/m^2 can be achieved at $<$10 V. High brightnesses of $\sim$4000, $\sim$10 000, and $\sim$500 cd/m^2 are obtained at a higher operating voltage $\sim$20 V for orange, green, and blue devices, respectively. The external EL efficiencies around the brightness level of 100 cd/m^2 for the blue, green, and orange devices are 0.5, 1.1, and 0.7%, respectively. The electrochemical potentials of the dyes used were measured and listed in Table I as those of the other materials described earlier. From the energy levels listed in Table I, the energy level alignment for all these devices is similar to that in Fig. 10, i.e., the HOMO/LUMO levels of all the emitting dopants lying within the bounds of the HOMO/LUMO levels of PVK and electron-transport molecules. In our previous work, we have demonstrated that three similar blue, green, and orange devices can be successfully integrated onto a single substrate using dry etching techniques [36]. The photograph of such an integrated three-color device is shown in Fig. 21.
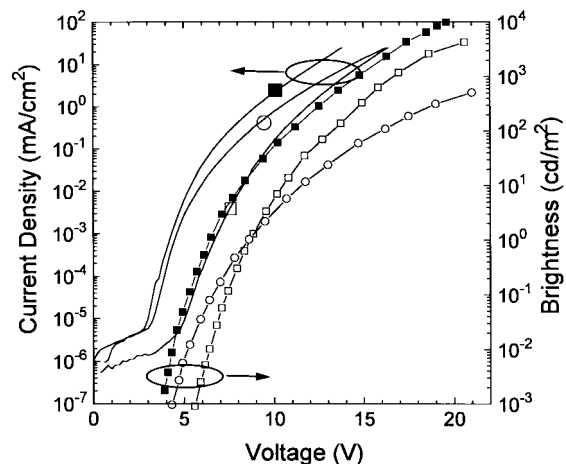
B. Effects of Cathode Metals on EL

In Fig. 22, the I–V curves of PVK:PBD:C6 (100:40:0.3) devices using Mg : Ag/Ag, Ag, Au, and Al as cathode contacts are shown. The external EL efficiencies are 1.1, 1.0, 0.1, and 0.01% for Mg : Ag/Ag, Ag, Au, and Al devices, respectively. There are several interesting observations in these I–V characteristics. First, for high current levels ($>$1 mA/cm^2), there is an inverse relationship between the voltage and EL efficiency. Also, there is no apparent trend for EL efficiency with the work functions of these metals, which are 3.7 eV, 4.3 (4.1–4.4) eV, 4.3 (4.2–4.7) eV, 5.1 (5.1–5.5) eV for Mg, Al, Ag, and Au, respectively [37]. It is usually believed that for organic light-emitting devices, lower work function metals give better device performance [38]. However, here we found that even air-stable Ag works nearly as well as reactive Mg : Ag (10 : 1) for this organic blend in terms of both I–V chracteristics and EL efficiency, in spite of the large difference in work functions, 4.3 eV of Ag versus 3.7 eV of Mg. Since, for different metals, the drop of EL efficiency comes along with the decrease of current for the same voltage, and the only variable here is the cathode metal, one concludes that a change in electron injection is the cause of both effects. Poorer electron injection leads to poorer EL efficiency and less recombination current. It is also clear that in devices with Mg : Ag or Ag contacts, the hole current is not dominant, otherwise the change of electron injection and electron current should not affect the total current. Therefore, with a proper choice of cathode, the blend films have bipolar injection and transport abilities. The lack of a corelation between device performance and metal work function implies an influence of the organic/metal interface, which strongly depends on the chemical properties and structure of the interface with a particular metal, not a general function of work function.

VI. CONCLUSION

Electroluminescent devices based on single-layer doped hole-transport polymer PVK were studied in detail. From the optical, electrical and electrochemical characterization of materials and devices, it is believed that charge carrier trapping is
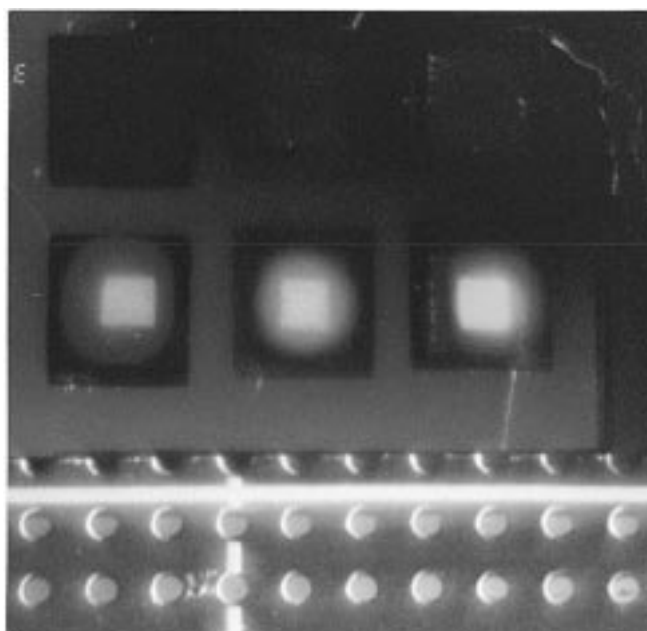
Fig. 21. A color photograph of working integrated orange, green, and blue devices on a same substrate. The picture was taken in the air under the illumination of a regular 60 W incandescent lamp. The exposure time was 1/60 s and the brightness of the orange, green, and blue devices were 100, 100, and 60 cd/m^2, respectively.
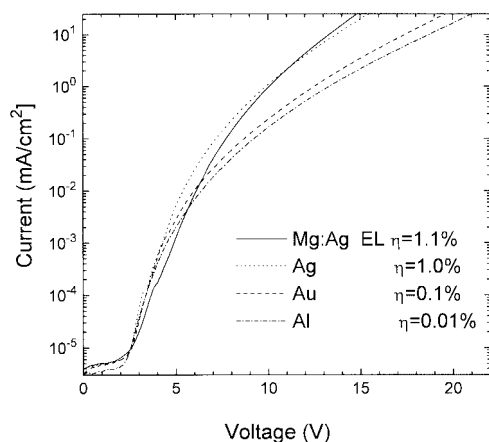

Fig. 22. Forward I–V characteristics of ITO/PVK:PBD:C6 $(100 : 40 : 0.3$ by wt.) /metal devices. The cathode metals are Mg:Ag/Ag, Ag, Au, and Al.

the mechanism responsible for the large enhancement of EL in both the PVK : fluorescent dopant system and PVK : electron-transport dopant : fluorescent dopant system. Our data support the conclusion that the excitons are formed by sequential capture of electrons and holes at the emitting centers, as opposed to the transfer of excitons from the carrier transporters to the emitting centers. To optimize the EL efficiency and the operating voltage of this class of devices, the addition of electron-transport materials and emitting materials has to be properly adjusted so that the bipolar carrier balance, optimal location of recombination zone and high radiative efficiency of emitting dopants can be achieved. The performance of PVK : electron-transport oxadiazole system does not have a clear dependence on the work functions of cathode metal contacts and even air-stable pure Ag can be used to build an efficient device with performance comparable to devices with

a reactive Mg : Ag alloy cathode. Using appropriate blends, devices with an external EL quantum efficiency >1%, a turn-on voltage of 3 V and a drive voltage of <10 V for 100 cd/m^2 can be achieved.

REFERENCES

[1] G. Gustafsson, Y. Cao, G. M. Treacy, F. Klavetter, N. Colaneri, and A. J. Heeger, "Flexible light-emitting diodes made from soluble conducting polymers," *Nature,* vol. 357, p. 477, 1992.
[2] E. Westerweele, P. Smith, and A. J. Heeger, "'Inverted' polymer light-emitting diodes on cylindrical metal substrates," *Adv. Mater.,* vol. 7, pp. 788–789, 1995.
[3] G. Yu, K. Pakbaz, and A. J. Heeger, "Optocoupler made from semiconducting polymers," *J. Electron. Mater.,* vol. 23, pp. 925–928, 1994.
[4] G. Yu, C. Zhang, and A. J. Heeger, "Dual-function semiconducting polymer devices: Light-emitting and photodetecting diodes," *Appl. Phys. Lett.,* vol. 64, pp. 1540–1542, 1994.
[5] H. H. Kim, R. G. Swartz, Y. Ota, T. K. Woodward, M. D. Feuer, and F. Papadimitrakapolous, "Prospects for silicon monolithic opto-electronics with polymer light-emitting diode," in *Proc. 1993 IEEE/LEOS Annu. Meet.,* pp. 202–203.
[6] N. Tessler, G. J. Denton, and R. H. Friend, "Lasing from conjugated-polymer microcavities," *Nature,* vol. 382, pp. 695–697, 1996.
[7] P. Yam, "Plastics get wired," *Sci. Amer.,* pp. 82–87, July 1995.
[8] A. J. Heeger and J. Long, Jr., "Optoelectronic devices fabricated from semiconducting polymers," *Opt. Photon. News,* pp. 23–30, Aug. 1996.
[9] P. May, "Light-emitting polymers: A technology for conformable graphic displays," in *SID Tech. Dig.,* May 1996, pp. 192–195.
[10] A. R. Brown, D. D. C. Bradley, P. L. Burn, J. H. Burroughes, R. H. Friend, N. Greenham, and A. Kraft, "Poly(p-phenylene vinylene) light-emitting diodes: Enhanced electroluminescent efficiency through charge-carrier confinement," *Appl. Phys. Lett.,* vol. 61, pp. 2793–2795, 1992.
[11] I. D. Parker, Q. Pei, and M. Marrocco, "Efficient blue electroluminescence from a fluorinated polyquinoline," *Appl. Phys. Lett.,* vol. 65, pp. 1272–1274, 1994.
[12] N. C. Greenham, S. C. Moratti, D. D. C. Bradley, R. H. Friend, and A. B. Holmes, "Efficient light-emitting diodes based on polymers with high electron affinities," *Nature,* vol. 365, pp. 628–630, 1993.
[13] J. Pommerehne, H. Vestweber, W. Guss, R. F. Mahrt, H. Bässler, M. Porsch, and J. Daub, "Efficient two-layer LED's on a polymer blend basis," *Adv. Mater.,* vol. 7, pp. 551–554, 1995.

[14] C. Zhang, H. von Seggern, K. Pakbaz, B. Kraabel, H.-W. Schmidt, and A. J. Heeger, "Blue electroluminescent diodes utilizing blends of poly(p-phenylphenylene vinylene) in poly(9-vinylcarbazole)," *Synth. Met.,* vol. 62, pp. 35–40, 1994.

[15] C. Zhang, H. von Seggern, B. Kraabel, H.-W. Schmidt, and A. J. Heeger, "Blue emission from polymer light-emitting diodes using nonconjugated polymer blends with air-stable electrodes," *Synth. Met.,* vol. 72, pp. 185–188, 1995.

[16] G. E. Johnson, K. M. McGrane, and M. Stolka, "Electroluminescence from single-layer molecularly-doped polymer films," *Pure Appl. Chem.,* vol. 67, pp. 175–182, 1995.

[17] J. Kido, M. Kohda, K. Okuyama, and K. Nagai, "Organic electroluminescent devices based on molecularly-doped polymers," *Appl. Phys. Lett.,* vol. 61, pp. 761–763, 1992.

[18] J. Kido, H. Shionoya, and K. Nagai, "Single-layer white-light-emitting organic electroluminescent devices based on dye-dispersed poly(N-vinylcarbazole)," *Appl. Phys. Lett.,* vol. 67, pp. 2281–2283, 1995.

[19] M. J. Marsella and T. M. Swager, "Regiochemical consequences in poly(2,5-pyridinium vinylene): Kekule$'$ and nonkekule$'$ conductive polymers," *Polym. Preprints,* vol. 33, no. 1, pp. 1196–1197, 1992.

[20] J. Tian, M. E. Thompson, C. C. Wu, J. C. Sturm, R. A. Register, M. J. Marsella, and T. M. Swager, "Luminescent properties of conjugated poly(p-pyridyl vinylene) and poly(p-pyridinium vinylene)," *Polym. Preprints,* vol. 35, no. 2, pp. 761–762, 1994.

[21] J. Tian, C. C. Wu, M. E. Thompson, J. C. Sturm, R. A. Register, M. J. Marsella, and T. M. Swager, "Electroluminescent properties of self-assembled polymer thin films," *Adv. Mater.,* vol. 7, pp. 395–398, 1995.

[22] J. Tian, C. C. Wu, M. E. Thompson, J. C. Sturm, and R. A. Register, "Photophysical properties, self-assembled thin films, and light-emitting diodes of poly(p-pyridylvinylene)s and poly(p-pyridinium vinylene)s," *Chem. Mater.,* vol. 7, pp. 2190–2198, 1995.

[23] C. C. Wu, C. I. Wu, J. C. Sturm, and A. Kahn, "Surface modification of indium tin oxide by plasma treatment: An effective method to improve the efficiency, brightness, and reliability of organic light-emitting devices," *Appl. Phys. Lett.,* vol. 70, pp. 1348–1350, 1997.

[24] N. C. Greenham, R. H. Friend, and D. D. C. Bradley, "Angular dependence of the emission from a conjugated polymer light-emitting diode: Implications for efficiency calculations," *Adv. Mater.,* vol. 6, pp. 491–494, 1994.

[25] N. C. Greenham, I. D. W. Samuel, G. R. Hayes, R. T. Phillips, Y. A. R. R. Kessener, S. C. Moratti, A. B. Holmes, and R. H. Friend, "Measurement of absolute photoluminescence quantum efficiencies in conjugated polymers," *Chem. Phys. Lett.,* vol. 241, pp. 89–96, 1995.

[26] S. E. Burns, N. C. Greenham, and R. H. Friend, "Modeling of optical interference effects in conjugated polymer films and devices," *Synth. Met.,* vol. 76, pp. 205–208, 1996.

[27] V. Choong, Y. Park, Y. Gao, T. Wehrmeister, K. Müllen, B. R. Hsieh, and C. W. Tang, "Dramatic photoluminescence quenching of phenylene vinylene oligomer thin films upon submonolayer Ca deposition," *Appl. Phys. Lett.,* vol. 69, pp. 1492–1494, 1996.

[28] S. Saito, T. Tsutsui, M. Era, N. Takada, C. Adachi, Y. Hamada, and T. Wakimoto, "Progress in organic multilayer electroluminescence devices," *Proc. SPIE,* vol. 1910, pp. 212–221, 1993.

[29] U. Lemmer, S. Karg, M. Scheidler, M. Deussen, W. Rieß, B. Cleve, P. Thomas, H. Bässler, M. Schwoerer, and E.O. Göbel, "Dynamics of photoexcitations in electric fields in PPV-diodes," *Synth. Met.,* vol. 67, pp. 169–172, 1994.

[30] R. Kersting, U. Lemmer, M. Deussen, H. J. Bakker, R. F. Mahrt, H. Kurz, V. I. Arkhipov, H. Bässler, and E. O. Göbel, "Ultrafast field-induced dissociation of excitons in conjugated polymers," *Phys. Rev. Lett.,* vol. 73, pp. 1440–1443, 1994.

[31] M. R. Andersson, M. Berggren, O. Inganäs, G. Gustafsson, J. C. Gustafsson-Carlberg, D. Selse, T. Hjertberg, and Wennerström, "Electroluminescence from substituted poly(thiophenes): From blue to near-infrared," *Macromolecules,* vol. 28, pp. 7525–7529, 1995.

[32] N. C. Greenham and R. H. Friend, "Semiconductor device physics of conjugated polymers," *Solid State Phys.,* vol. 49, pp. 1–148, 1995.

[33] M. Stolka, "Photoconductive polymers," in *Special Polymers for Electronic & Optoelectronics,* J. A. Chilton and M. T. Goosey, Eds. London, U.K.: Chapman & Hall, 1995.

[34] H. Tokuhisa, M. Era, T. Tsutsui, and S. Saito, "Electron drift mobility of oxadiazole derivatives doped in polycarbonate," *Appl. Phys. Lett.,* vol. 66, pp. 3433–3435, 1995.

[35] W. D. Gill, "Drift mobilities in amorphous charge-transfer complexes of trinitrofluorenone and poly-n-vinylcarbazole," *J. Appl. Phys.,* vol. 43, pp. 5033–5040, 1972.

[36] C. C. Wu, J. C. Sturm, R. A. Register, and M. E. Thompson, "Integrated three-color organic light-emitting devices," *Appl. Phys. Lett.,* vol. 69, pp. 3117–3119, 1996.

[37] D. R. Lide, Ed., *CRC Handbook of Chemistry and Physics.* Boca Raton, FL: CRC, 1991.

[38] I. D. Parker, "Carrier tunneling and device characteristics in polymer light-emitting diodes," *J. Appl. Phys.,* vol. 75, pp. 1656–1666, 1994.

Chung-Chih Wu was born in Taiwan, R.O.C., on February 22, 1968. He received the B.S. degree from National Taiwan University, Taipei, in 1990, and the M.A. degree from Princeton University, Princeton, NJ, in 1994, both in electrical engineering. He is currently pursuing the Ph.D. degree in electrical engineering at Princeton University, where he is studying thin-film light-emitting devices based on polymeric and molecular organic semiconductors and their applications for flat-panel displays.

From 1990 to 1992 he was an ROTC Officer at R.O.C. Naval Communications and Electronics School, Kaohsiung, Taiwan, where he taught radar and communication systems.

James C. Sturm (M'80–SM'96) was born in Berkeley Heights, NJ, in 1957. He received the B.S.E. degree in electrical engineering and engineering physics from Princeton University, Princeton, NJ, in 1979, and the M.S.E.E. and Ph.D. degrees from Stanford University, Stanford, CA, in 1981 and 1985, respectively.

In 1979, he joined Intel Corporation, Santa Clara, CA, as a Microprocessor Design Engineer. In 1981, he was a Visiting Engineer at Siemens Company, Munich, Germany. In 1986, he joined the faculty of Princeton University in the Department of Electrical Engineering, where he is currently a Professor. From 1994 to 1995, he was a von Humboldt Fellow at the Institut fuer Halbleitertechnik at the University of Stuttgart, Germany. He has worked in the fields of silicon-based heterojunctions, 3-D integration, silicon-on-insulator, and flat-panel displays. His current research interests include silicon-germanium and related heterojunctions, macroelectronics, and organic semiconductors.

Dr. Sturm is a member of the American Physical Society and the Materials Research Society, and was a National Science Foundation Presidential Young Investigator. He served on the organizing committee of IEDM from 1988 to 1992, as a Symposium Leader for the Materials Research Society in 1987 and 1995, and on the SOS/SOI, DRC, and EMC conference committees. In 1996 and 1997, he was the Technical Program Chair and General Chair of the IEEE Device Research Conference.

Richard A. Register received the B.S. degree in chemistry in 1983, the B.S. degree in chemical engineering in 1984, and the M.S. degree in chemical engineering practice in 1985, all from the Massachusetts Institute of Technology, Cambridge, and the Ph.D. degree in chemical engineering in 1989 from the University of Wisconsin, Madison.

In 1990, he joined the Chemical Engineering Department at Princeton University, Princeton, NJ, where he is currently Associate Professor, as well as a member of the Princeton Materials Institute and the Center for Photonic and Optoelectronic Materials. His research interests are in the structure and properties of complex polymeric materials, particularly block copolymers, polymer blends, semicrystalline polymers, and ionomers; rheology of associating polymers; fiber-reinforced thermoplastics; and electroluminescent polymers.

Dr. Register received the Unilever Award from the American Chemical Society in 1992, and has also been named an NSF Young Investigator and a DuPont Young Professor.

Jing Tian received the B.S. degree in chemistry from the Shanghai University of Science and Technology, Shanghai, China, and the Ph.D. degree in polymer science from Drexel University, Philadelphia, PA, in 1993. From 1994 to 1995, she was a Postdoctoral Fellow in the Department of Chemistry, Princeton University, Princeton, NJ, where she carried out research on fabrication and characterization of polymeric light-emitting devices.

Since 1995, she has been with Raychem Corporation, Menlo Park, CA, as a Staff Research Scientist. She is currently working in the area of Lipolymer rechargeable batteries.

Elena P. Dana received the M.S. degree from the Biological Faculty of Moscow State University, Moscow, Russia, and the Ph.D. degree from the Institute of Photosynthesis of the Russian Academy of Sciences, Minsk, Russia, in 1991.

She conducted her postdoctoral research at the University of Quebec, Trois-Rivieres, P.Q., Canada, Princeton University, Princeton, NJ, and the University of Southern California, Los Angeles. Her research interests include electrochemistry of biomolecules, electrochemical processes in thin films at the electrodes, and photochemical energy conversion in photosynthesis and in model systems.

Mark E. Thompson received the B.S. degree in chemistry from the University of California, Berkeley, in 1980, and the Ph.D. degree in chemistry from the California Institute of Technology, Pasadena, in 1985.

After completing his graduate work, he took a S.E.R.C. postdoctoral fellowship in the Inorganic Chemistry Laboratory, Oxford, U.K. In 1987, he joined the faculty of the Chemistry Department at Princeton University, Princeton, NJ, as an Assistant Professor. In August 1995, he joined the Department of Chemistry at the University of Southern California, Los Angeles, where he is currently an Associate Professor. His research program is aimed at understanding the optical, electronic, and catalytic properties of novel organic and metal-organic materials.